

Thermal Annealing of Gold Thin Films on the Structure and Surface Morphology Using RF Magnetron Sputtering

Moniruzzaman Syed¹, Caleb Glaser², Cameron Hynes¹ and Muhtadyuzzaman Syed³

1. Division of Natural and Mathematical Sciences, Lemoyne-Owen College, Memphis, TN 38126, USA

2. Sandia National Laboratories, Albuquerque, NM 87185, USA

3. Department of Electrical and Computer Engineering, Purdue University, West Lafayette, IN 47907, USA

Abstract: Gold (Au) thin films were deposited on SiO₂ substrate under argon (Ar) gas environment using RF (radio frequency) magnetron sputtering at room temperature for various deposition times. These samples have been annealed at the temperature range of 250–450 °C. The change of the structural and surface morphological properties of both as-deposited and annealed films has been studied using an AFM (atomic force microscope), XRD (X-ray diffraction) and Raman scattering. The improvement of crystallinity was observed at the annealing temperature of 350 °C and degradation was found thereafter. In agreement with XRD and Raman measurements, both crystallite size and crystalline volume fraction were found to be increased having maximum at 350 °C and decreased afterward. This result can be explained by simple kinetic theory where sticking probabilities, Au structures agglomerated on SiO₂ surfaces and surface coverage of Au atoms must be considered. Moreover, it can also be explained by the occurrence of two competing phenomena like roughening induced grain growth and smoothing induced inhibition of grain growth with increasing annealing time. Growth mechanisms are also discussed.

Key words: Gold, annealing and magnetron sputtering.

Nomenclature

rms:	Roughness
Φ:	Deposition time
ρ:	Crystalline volume fraction

Greek letters

δ:	Crystallite size
λ:	Wavelength
θ:	Angle
σ _i :	Intrinsic stress

1. Introduction

Gold (Au) thin films have a wide range of applications in many fields and may be used for memory storage, energy harvesting [1-3] and storage, nanosensors, optics, corrosion prevention, ware

protection and biosensing devices [4-5]. Au thin films on SiO₂/or Silicon has been studied for interconnection in IC (integrated circuit) fabrication, because it has a high conductivity. Various approaches such as sputtering, pulsed laser deposition, vacuum evaporation and molecular beam epitaxy have been used for thin film growth. Deposition technique, properties of substrate, adsorbed atoms and their interaction strength with the substrate surface are playing very important role on the growing rate, micro structure and morphology of the thin metal films. In physics of thin films and also in a wide range of technological applications, initial phase of the film growth and its morphology is a persisting problem. Venables et al. [1] have observed and discussed three basic mechanisms of the film growth. Au thin films are currently being studied more closely for many critical applications, as they are highly conductive and

Corresponding author: Moniruzzaman Syed, Ph.D., associate professor of physics, research field: thin film research.

yet not easily oxidized. It is also exhibiting interesting physicochemical properties of gold nanoparticles. Therefore, it is necessary to understand the structural, surface morphology and growth mechanisms of film at early stage of deposition on various substrates. The structural properties of films are showing crucial role on the film quality, which may affect its optical properties as well as the sensing capabilities of the device. Many research groups published the Au deposition [7-9] but there is no report on the systematic investigation of the annealing effects on the structural and surface morphological properties of Au film on SiO_2 substrate. Therefore in this study, we deposited the Au thin film on glass substrate by RF (radio frequency) magnetron sputtering at room temperature and investigated the effect of annealing temperature on the structural property of Au thin layers. Raman scattering, XRD (X-ray diffraction) and AFM (atomic force microscope) methods have been

used for the study of growth, morphology and the structural properties of thin gold layers.

2. Experimental Setup

Magnetron sputtering is a PVD (physical vapor deposition) technique and the depositions are performed at low pressure in a versatile system. The method is reliable, the results can easily be reproduced and the technique is frequently used for large-scale coatings of thin films. Sputtering means that atoms from a target are knocked out by energetic ions, the released atoms are deposited onto a substrate and a layer is built up.

All SiO_2 substrates were cleaned by acetone, isopropanol, and deionized water for 15 minutes respectively (Table 1). After allowing the substrates to air dry, tape was covered to a small area of glass substrates to form a mask for deposition in order to measure the film thickness. Deposition was carried out

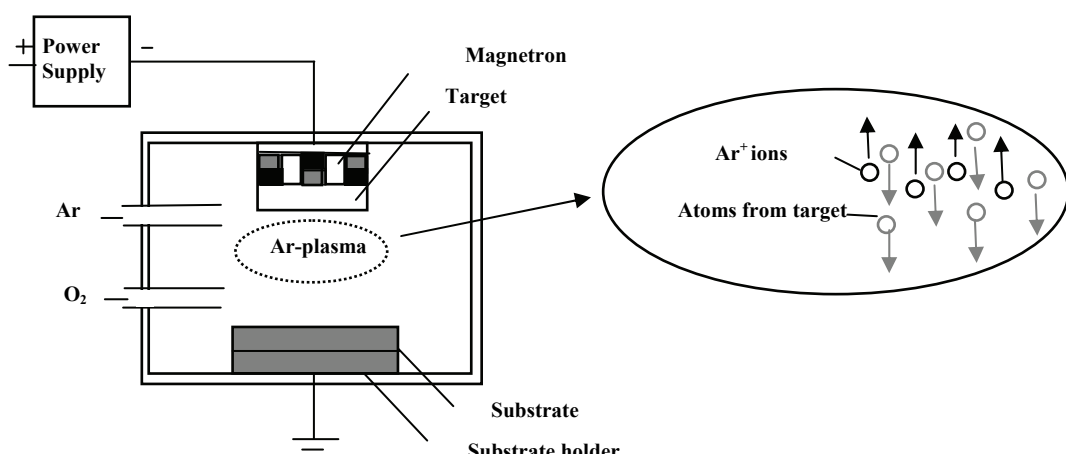


Fig. 1 Overview of the schematic diagram of magnetron sputtering used in this experiment.

Table 1 Substrates cleaning conditions.

Substrate	Acetone	Isopropanol	DI water
	min	min	min
Glass	15	15	15

Table 2 Gold thin film deposition conditions.

Substrate	Gas pressure	Current	Voltage
	mT	mA	V
Glass	100	5	5

Thermal Annealing of Gold Thin Films on the Structure and Surface Morphology Using RF Magnetron Sputtering

in a 15 sccm of argon (Ar) (99.99% purity) gas atmosphere by supplying 90 W of RF power with frequency of 13.56 MHZ. The Au thin film was grown at RT and pressure of 100 mT, respectively, for deposition time of 15, 20, 25, 30 and 35 minutes. After the RF magnetron sputtering, the samples were annealed in a furnace using quartz tube reactor at the temperature in the range of 250-450 °C in an Ar ambient. The deposition rate for each sample was determined by measuring the thickness of the film using an Ambios XP-1 profilometer. The AFM is a scanning probe microscope. It works by scanning an extremely fine probe on the end of a cantilever across the surface of a material, profiling the surface by measuring the deflection of the cantilever. This allows a 2D/3D profile of the surface to be produced at magnifications over one million times, giving much more topographical information than optical or scanning electron microscopes. Its limitation is that the surface to be observed needs to be very flat or the tip will crash into the “hills” as it is scanned. The microscope can run in two modes: contact and close contact. Contact mode scans the probe across the surface, keeping a constant force between tip and sample, maintained by a feedback control. The amount of movement required to keep the constant force is then used to create the image. Close contact mode, often called tapping mode, uses a vibrating cantilever. Simple height data can be obtained from the changes in Z-axis displacement, but phase data can also be obtained. AFM images were recorded with a Veeco CP-II AFM to analyze the topography of the film surface. Images taken with the AFM were analyzed using Gwyddion software. Tapping mode was used in this experiment. The root mean square (rms), also known as the quadratic mean, is a statistical measure of the magnitude of a varying quantity. It is especially useful when variants are positive and negative.

It can be calculated for a series of discrete values or for a continuously varying function. Its name comes

from its definition as the square root of the mean of the squares of the values.

$$\text{rms} = \sqrt{\frac{(Z_1 - Z_{\text{ave}})^2}{N}} \quad (1)$$

The XRD measurements were carried out using an XRD apparatus (Shimadzu XD-D1), employing a diffractometer with a slit width of 0.1 mm set at the front of the detector. Diffractograms were registered at the angle range of $2\theta = 10^\circ$ - 85° . The average grain size, δ in the depth direction was estimated from the half-width value of the X-ray spectra by the Scherrer formula,

$$\delta = 0.9 \times \lambda / B \times \cos\theta \quad (2)$$

where B is the corrected width: $B = (B_S - B_M)$, where B_S is the half width values measured and B_M the width due to instrumental broadening. Wavelength of the x-ray used is $\lambda = 1.5418 \text{ \AA}$. The structural properties were also characterized by Raman scattering measurements. The FWHM (full width half maximum) of the films was estimated from the Raman spectra. The stress was estimated from changes in the curvature of the substrate/film system using Stoney's formula.

3. Experimental Results

3.1 Evaluation of Structural Properties Based on XRD Measurements

All Au samples, without annealing and with annealing at different temperatures were shown θ - 2θ patterns of face-centered cubic phase with dominant (111), (200), (220) and (311) diffraction peaks. However, the relative intensities of (111), (200) and (311) diffraction peaks become noticeable after thermal annealing at 350 °C. Figs. 2a and 2b show the $\langle 111 \rangle$ XRD relative intensity, I_X , and the $\langle 111 \rangle$ Crystallite size, $\langle \delta \rangle$, respectively, for Au films on glass substrates as a function of deposition time. Both I_X and $\langle \delta \rangle$ values are found to increase monotonically with increasing deposition time on glass substrates condition, and the following relationship is obtained:

$I_X \propto <\delta>^{1.7}$ ($= <\delta>^2$). However, we have observed the relationship, $I_X \propto <\delta>^3$, for Au films on glass substrates. The mechanism behind such relationship between I_X and $<\delta>$ is unknown.

Fig. 2b shows the crystallite size, $<\delta>$ of Au thin films on glass substrates as a function of deposition time. As shown in this diagram, $<\delta>$ was found to be increased as deposition time increasing at annealed temperature of 350 °C, maximum $<\delta>$ was estimated

on glass substrates, $<\delta> = 40$ nm. The impact of the deposition time on the crystallite size on various substrates revealed that higher sputtering yields resulted in the formation of bigger gold particles. The observed deposition rate data (Fig. 4a) have been suggested that controlled deposition time variations enable to tailor the coherent diffraction domain size [10], which determines the electronic-optical properties of Au system.

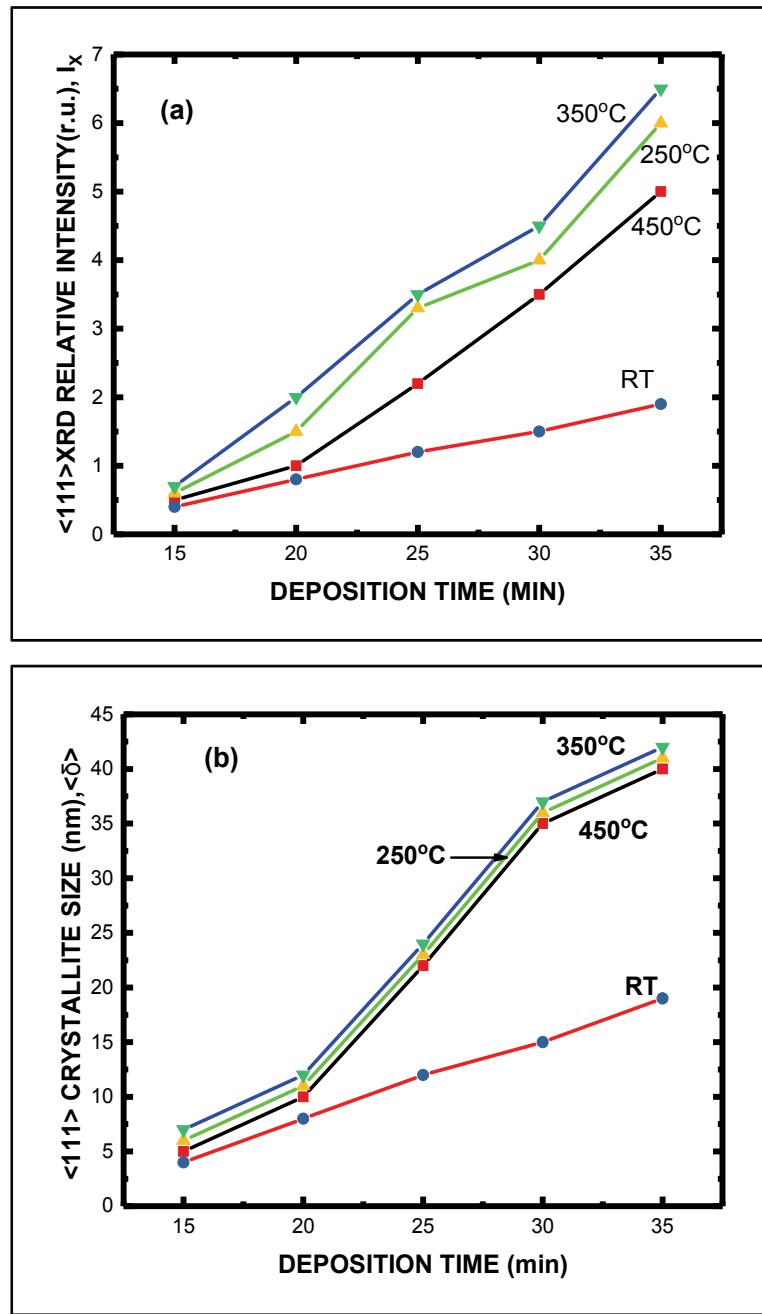


Fig. 2 (a) $<110>$ XRD relative intensity and (b) $<111>$ crystallite size as a function of deposition time on glass substrates.

3.2 Evaluation of Structural Properties Based on Raman Scattering Measurements

Figs. 3a and 3b show the $1,574\text{ cm}^{-1}$ Raman intensity and FWHM of Raman spectra of Au thin film deposited on glass substrates as a function of deposition time.

As revealed in Fig. 3a, $1,574\text{ cm}^{-1}$ Raman intensity increases as deposition time increases, however, the overall intensity is getting higher for the films deposited on glass substrates at $350\text{ }^{\circ}\text{C}$. As shown in Fig. 3b, the value of the FWHM, estimated from $1,574\text{ cm}^{-1}$ Raman spectra is found to be decreased with increasing the deposition time on glass substrates having the lowest value at $350\text{ }^{\circ}\text{C}$. Similarly, Fig. 3c shows the variation of peak frequency as a function of deposition time under various annealed temperature. The Raman shifts are controlled by vibration of the electronic polarization for constituents in the films which depends on the bonding structure such as atomic distance. So, the value of the FWHM will, in general, broaden as the magnitude of the lattice strain is widely distributed in a film. On the other hand, if the atomic distance is uniformly strained, the width of the Raman spectra will be unchanged, but its peak frequency should shift. Fig. 3c shows the peak frequency of $1,574\text{ cm}^{-1}$ component as a function of deposition time on glass substrates. As Au films on glass substrates, it is found that the peak shifts toward a lower frequency side with increasing deposition time. Such Raman peak shifts would be related to a change in the stress of the films as discussed below

3.3 Evaluation of Structural Properties Based on Stress Measurements

Fig. 4a shows the stress of Au films deposited on glass substrates as a function of deposition time under various annealed temperatures. In this diagram, the positive values of stress denote tensile stress. The values of stress for Au films on glass substrates are always lower with increasing deposition time. At

$350\text{ }^{\circ}\text{C}$, on glass substrate the lowest stress, $\sigma_G = 10 \times 10^8\text{ N/m}^2$ was observed. The measured stress is composed of two different types of stress: one is the stress, σ_t , caused by the thermal expansion mismatch between the film and the substrate, and the other is the intrinsic stress, σ_i , controlled by the growth process of the film. The value of σ_t can be given by

$$\sigma_t = (\alpha_S - \alpha_G) \Delta T Y / (1-v) \quad (3)$$

where α_S and α_G are the thermal expansion coefficient for the Au film and the substrate, respectively. The symbols Y and v are Young's modulus and the Poisson ratio for Au film. The value ΔT is assumed as the difference between the deposition temperature (Room temperature = $300\text{ }^{\circ}\text{C}$) of the films and room temperature at which the stress was measured. As described, shifts in the Raman peak frequency would be related to change in the stress of the films. A positive Raman-peak shift can be interpreted as indicating an increase in the compressive stress or a decrease in the tensile stress. A negative Raman peak shift may be caused by a deterioration of the structural properties and may be related to a change in the robustness in the Au network. Fig. 4b shows the deposition rate as a function deposition time under various annealed temperature. Over all deposition rate was found to be decreased with increasing deposition time. At $350\text{ }^{\circ}\text{C}$ annealed temperature, deposition rate was found to be the lowest. This result is consistent with the above results.

Fig. 4b shows the dependence of the deposition rate of Au thin films as a function of deposition time on glass substrates under various annealed temperature. On glass substrates deposition rate increases sharply with increasing deposition time and $350\text{ }^{\circ}\text{C}$ has been shown the lowest deposition rate as observed in Fig. 4b.

It is evident that the overall deposition rate on glass substrate is slower at $350\text{ }^{\circ}\text{C}$. Gold layers deposited for the longest deposition times are discontinuous, i.e., composed of separated gold islands. Observed evolution of the deposition rate on the glass substrate

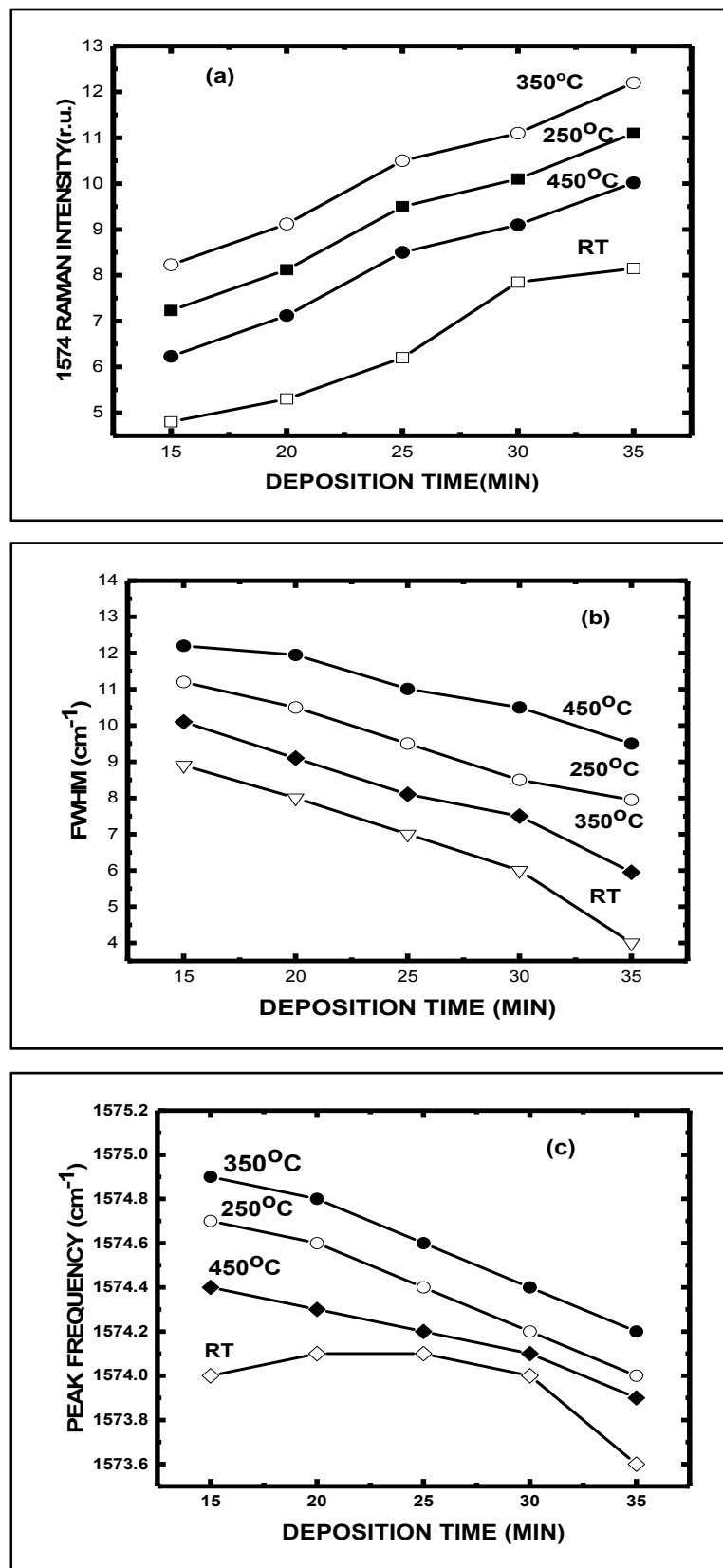


Fig. 3 (a) $1,574 \text{ cm}^{-1}$ Raman intensity, (b) FWHM, and (c) peak frequency on glass substrates as a function of deposition time under various annealed temperature.

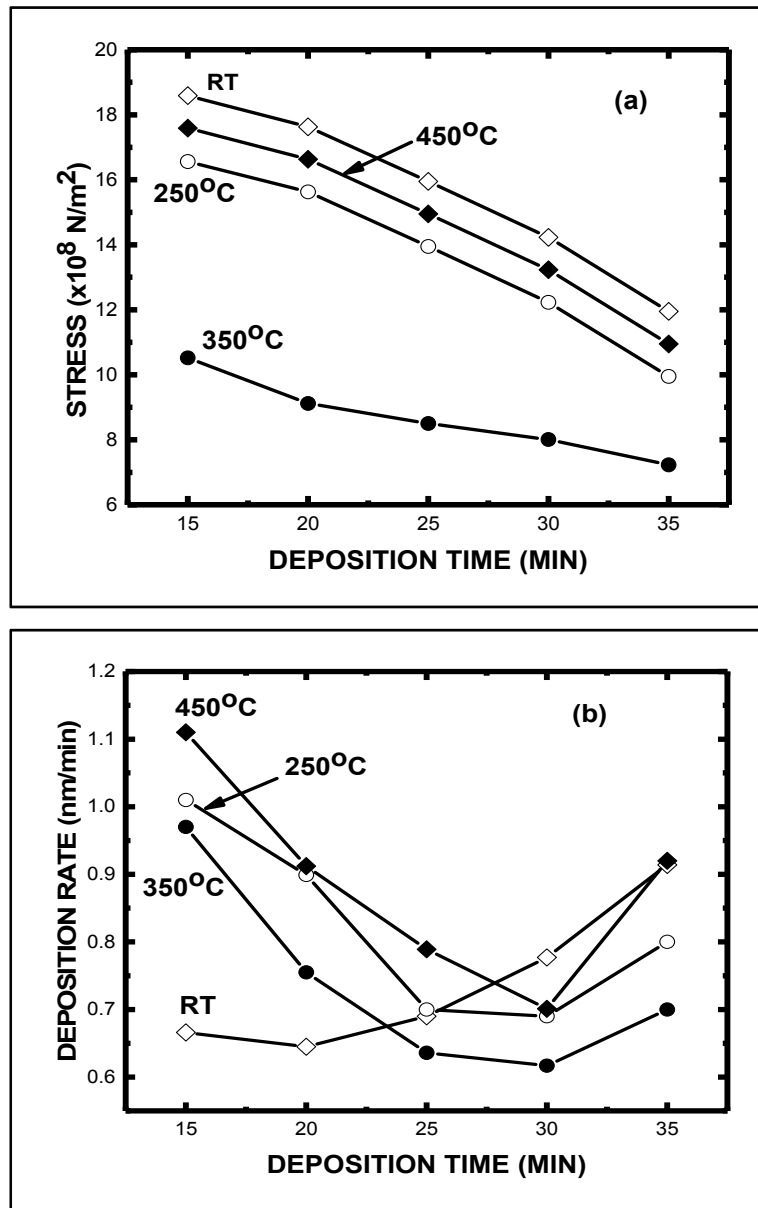


Fig. 4 Dependence of (a) stress and (b) deposition rate of Au films on glass substrates as a function of deposition time under the various annealed temperature.

may be due to different sticking probabilities of gold atom capture on the bare glass substrate and already created gold islands. These results are consistent with the AFM results shown in Fig. 5.

3.4 Evaluation of Surface Morphology Based on AFM Measurements

Fig. 5 shows AFM micro graphs of the Au films deposited on glass substrates as a function of deposition time under various annealed temperature (a)

RT, (b) 350 °C and (c) 450 °C. In these diagrams, the degree of surface roughness is the root mean square (rms) value of the roughness heights. Uniformly distributed Au grains were observed for the films (rms = 1.47 nm) at RT. However the presences of polygonal-like islands with a larger aspect ratio (height/width) with respect to sample 5a were noticed at 350 °C. Moreover the later displayed the presence of three dimensional individual Au particles were perceived at 450 °C. Finally, at 350 °C, the Au

particles are pulled together from the nearest surface to form the cluster and/or island type structure ($\text{rms} = 5.25 \text{ nm}$) because Au has a rather high surface tension [4-7].

Fig. 6 shows the rms value by AFM as a function of deposition time under various annealed temperatures. Glass surface exhibits higher surface roughness compared to Si surface. A rather complex surface morphology is observed on the gold-covered glass. The presence of isolated gold grains of various sizes is observed for 450°C . With increasing deposition time the mean size and the density of these grains increase, but the initial size differences are gradually smeared

out. The later effect is reflected in the evolution of the surface roughness which increases rapidly in initial deposition stages. With increasing annealed temperature, the gold layer becomes electrically conductive. The appearance of the gold grains and their growth may be due to the above-mentioned preferential capture of the incoming gold atoms on the already existing gold islands or to surface diffusion of deposited gold atoms and their aggregation into larger grains.

It may be concluded that the initial morphology of the substrate affects the morphology of the deposited Au layer significantly.

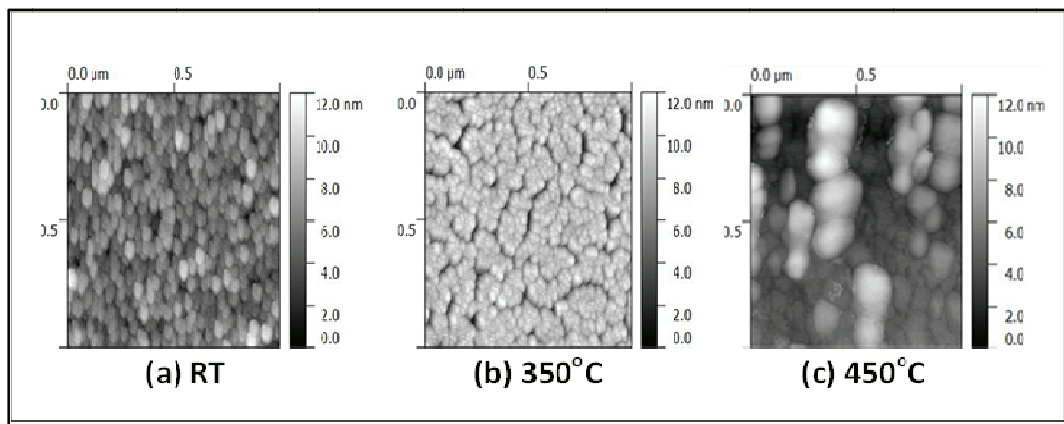


Fig. 5 AFM micrographs of Au thin films on glass substrates as a function of deposition time under various annealed temperature.

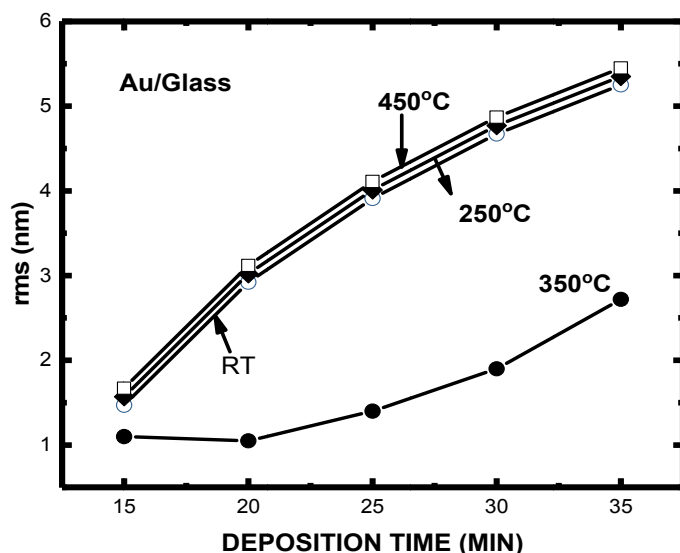


Fig. 6 AFM surface roughness (rms) of Au thin films on glass substrates as a function of deposition time under various annealed temperature.

Thermal Annealing of Gold Thin Films on the Structure and Surface Morphology Using RF Magnetron Sputtering

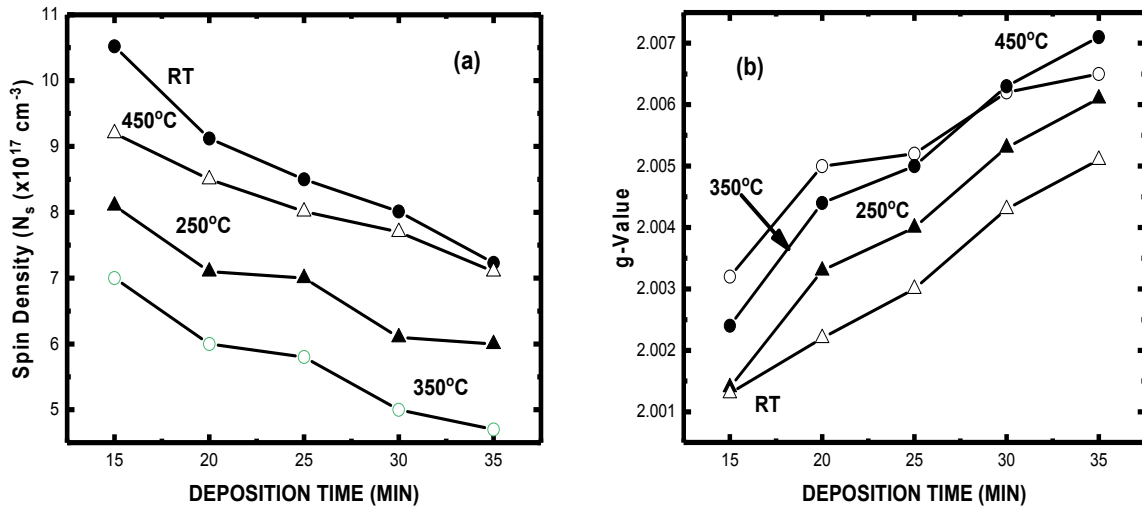


Fig. 7 (a) Spin density and (b) g-value of gold thin films on glass substrates as a function of deposition time under various annealed temperatures.

3.5 Analysis of ESR (Electron Spin Resonance) Measurements

Figs. 7a and 7b show the ESR spin density, N_s and g-value for Au films on glass substrates as a function of deposition time under various annealed temperatures. The measurements were performed within a few days of the deposition. The value of N_s monotonically decreases, as deposition rate increases on glass substrates. On the other hand, g-value was found to be increased as deposition rate increasing for glass substrates.

4. Growth Mechanisms of Au Layers at Early Deposition Stages

Au thin films were prepared using RF magnetron sputtering on glass substrates under various annealed temperatures in order to understand the structural and surface morphology of Au films. Several mechanisms may jointly be responsible for determining the structural and morphological properties of films should be considered [11, 12]: (1) change in the surface morphology of the substrate surface, (2) change in the deposition rate, (3) change in surface migration of adsorbates, caused by different Au coverage of the growth surface, and (4) removal of

strained surface bonds. As shown in Figs. 2 and 3, Au grains can be deposited on glass substrate with a rough surface showing highly roughened, due, most likely to the increased $\langle\delta\rangle$ values. Contrasting results have also been observed for uniform Au films on silicon substrates with a smooth surface used in the present study.

The results of this study showed a significant difference in the structure of Au-films depending on if the substrate material was conducting or non-conducting. Therefore gold film coalescence was studied on two kinds of substrates. Films were deposited on those substrates with identical deposition conditions as a function of deposition time. AFM micrographs show Au films on non-conducting substrates (glass) have larger coalescence at 350 °C annealed temperature. For non-conducting substrates, homogenous structure changes to cluster-type structures with increasing sputtering time. On the other hand, for conducting substrates (silicon), a uniform worm-like structure with micro-voids has changed to homogenous structures [13-17]. While the deposition on glass substrate proceeds with increasing deposition time and in the case of the Si substrate, the deposition in the initial stages of the layer growth proceeds with significantly decreasing deposition rate.

It should be noted that the gold layers deposited for the shortest deposition times are irregular. Observed evolution of the deposition rate on the glass substrate may be due to different probabilities of gold atom capture on the bare glass substrate and already created gold islands. It is suggesting a predominance of vertical growth with respect to the lateral one. These results could be explained taking into account that larger Au crystallites were formed at higher deposition time, and hence, higher sputtering yields. Their low surface mobility likely resulted in a low coverage of the glass surface and in a minor density of nucleation sites. Due to the high sputtering yields, these nuclei grew vertically more than laterally, resulting in the formation of cluster-like Au/glass system. Conversely, lower T_d and lower sputtering yields produced the initial deposition of crystallites with a smaller size. Their higher surface mobility likely favored the lateral growth and agglomeration that, under the present conditions, can be comparable or higher than the vertical one [17-20]. These results were consistent with the initial formation of a thin layer completely covering the surface and with the surface morphology. Although we believed that mechanisms 1&2 contribute predominantly to the control of the structural properties, mechanism 3 and/or 4 may also be contributing factors.

5. Conclusion

In order to examine the structural and surface morphology of gold layers sputtered onto glass substrates as a function of the deposition time under annealed temperature, the deposition rate on glass substrate is monotonously increasing as a function of deposition time as could be expected. The deposition rate on the silicon substrate is decreasing with $[T_S]$. For the glass substrate, however, the deposition rate is low for short sputtering times having discontinuous gold coverage and with increasing deposition time having more homogenous coverage; it increases to a value comparable with that found on the silicon

substrate. At deposition time = 35 min, $\langle\delta\rangle = 40$ nm, low stress, low spin density and higher g-value were observed. The observed dependence can be explained by different sticking probabilities of gold atoms on the bare glass substrate and on regions with gold coverage. AFM images taken on bare substrates and those coated with gold for different deposition times show great differences in the morphology of the gold layers deposited on both substrates. On the silicon substrate, rather homogenous gold layers are observed, the surface morphology of which has only little changes with increasing sputtering time. At deposition time = 35 min on silicon substrate, $\langle\delta\rangle = 20$ nm and high stress (9.95×10^8 N/m²) were obtained. At the deposition stage roughly corresponding to the outbreak of layer electrical conductivity, a worm-like structure in the gold layer is formed, and at later deposition stages, a globular layer structure is observed. On the glass substrate, however, the presence of isolated gold grains of various sizes is observed for short deposition times. With increasing deposition time, the mean size and the density of these grains increase, but the initial differences in the grain size are gradually smeared out. XRD, stress and Raman scattering results are well consistent with the AFM results. Present results contribute to a better understanding of initial stages of the formation of metal layers on different substrates. The results of such examinations suggest that mechanism (1&2) along with mechanism (3) and/or (4), as described above, may be effective in controlling the structure and morphology process of Au films. The results can be of interest for specialists developing meta-materials, photonic crystal structures, and nanostructured materials with enhanced biocompatibility. This study will contribute to the potential applications of Au/SiO₂ to the interconnection in IC fabrication.

Acknowledgements

Authors acknowledge the support from Drs. Anura Goonewardene and Indrajith Senevirathne of Lock

Thermal Annealing of Gold Thin Films on the Structure and Surface Morphology Using RF Magnetron Sputtering

Haven University of Pennsylvania for AFM assistance. Authors would also be grateful to the monitory support from Lock Haven University Nanotechnology Program, NSF-STEM Awards #0806660. Special thanks go to Dr. Sherry Painter of LeMoyne-Owen College for her support.

References

- [1] Venables, J. A., Spiller, G. D. T., and Hanbucken, M. 1984. "Nucleation and Growth of Thin Films." *Rep. Prog. Phys.* 47: 399-459.
- [2] Lee, S., Hong, J., and Oh, S. H. 1997. "Inversion of Temperature-Dependent in Situ Ellipsometry Constants of Au Thin Films." *Surf. Coat. Technol.* 94/95: 368.
- [3] Dishner, M. H., Ivey, M. M., Gorer, S., and Hemminger, J. C. 1998. "Preparation of Gold Thin Films by Epitaxial Growth on Mica and the Effect of Flame Annealing." *J. Vac. Sci. Technol. A* 16 (6): 3295-300.
- [4] Chang, J. F., Young, T. F., Yang, Y. L., Ueng, H. Y., and Chang, T. C. 2004. "Silicide Formation of Au Thin Films on (1 0 0) Si during Annealing." *Mater. Chem. Phys.* 83: 199.
- [5] Netterfield, P., Martin, P. J., Sainty, W. G., Duffy, R. M., and Pacey, C. G. 1985. "Characterization of Growing Thin Films by in Situ Ellipsometry, Spectral Reflectance and Transmittance Measurements, and Ion-scattering Spectroscopy." *Pacey Sci. Instrum.* 56: 1995-2003.
- [6] Glick, F. J., and Pern, S. H. 2003. "Adhesion Strength Study of EVA Encapsulates on Glass Substrates." National Center for Photovoltaics and Solar Program Review Meeting (National Renewable Energy Laboratory).
- [7] University of Cambridge, Department of Physics. 2010. "Crystallization of Au Thin Films on Si-Based Substrates by Annealing for Self-assembly Monolayers."
- [8] Wang, C. M., Ma, L. Y., and Su, M. 2009. "Polyelectrolyte Multilayers Stabilized Plasmonic Nanosensors." *IEEE Sensors 2009 Conference*, 338.
- [9] Baranov, I., Brunelle, A., Della-Negra, S., Jacquet, D., Kirillov, S., Le Beyec, Y., Novikov, A., Obonorskii, V., Pchelintsev, A., Wien, K., and Yarmiychuk, S. 2002. "Sputtering of Nanodispersed Targets of Gold and Desorption of Gold Nanoclusters (2-100 nm) by 6 MeV Au 5 Cluster Ions." *Nuclear Instruments and Methods in Physics Research B* 193 (1): 809-15.
- [10] Dixon, M., Daniel, T. A., Hieda, M., Smilgies, D. M., Chan, M. H. W., and Allara, D. L. 2007. "Preparation, Structure and Optical Properties of Nanoporous Gold Thin Films." *American Chemical Society (Langmuir)* 23 (5): 2414-22.
- [11] Dash, P., Rath, H., Dash, B. N., Mallick, P., Basu, T., Som, T., Singh, U. P., and Mishra, N. C. 2012. "Evolution of microstructure and Surface Topography of Gold Thin Films under Thermal Annealing." *AIP* 46 (10).
- [12] Singh, S. P., Arya, S. K., Pandey, P., and Malhotra, B. D. 2007. "Cholesterol Biosensor Based on Rf Sputtered Zinc Oxide Nanoporous Thin Film." *Applied Physics Letters* 91 (6): 063901.
- [13] Garnaes, J., Christensen, F. E., Besenbacher, F., Laegsgaard, E., and Stensgard, I. 1999. "Fabrication of Nano-Structured Gold Films by Electrohydrodynamic Atomization." *Opt. Eng.* 29: 666.
- [14] Campbell, D. J., Herr, B. R., Hulteen, J. C., Van Duyne, R. P., and Mirkin, C. A. 1996. "Synthesis of Thiol-Derivatized Ferrocene-Porphyrins for Studies of Multibit Information Storage." *J. Am. Chem. Soc.* 118: 10211.
- [15] Lee, S., Hong, J., and Oh, S.-H. 1997. "Nucleation and Growth of Gold Nanoparticles Deposited by RF-Sputtering: An Experimental Study." *Surf. Coat. Technol.* 94/95: 368.
- [16] Dishner, M. H., Ivey, M. M., Gorer, S., and Hemminger, J. C. 1998. "CuAg Nanostructure Surface Coexistence and Ag Surface." *J. Vac. Sci. Technol. A* 16: 3295.
- [17] Netterfield, P., Martin, P. J., Sainty, W. G., Duffy, R. M., and Pacey, C. G. 1985. "Characterization of Growing Thin Films by in Situ Ellipsometry, Spectral Reflectance and Transmittance Measurements, and Ion-Scattering Spectroscopy." *Sci. Instrum.* 56: 1995.
- [18] Anders, A., Anders, S., Brown, I., and Ivanov, I. C. 1994. "Advances and Applications in the Metallography and Characterization of Materials and Microelectronic Components." *Mater. Res. Soc. Symp. Proc.* 316: 833.
- [19] Lee, S. C., Hwang, N. M., Yu, B. D., and Kim, D. Y. 2002. "Assembly and Electronic Applications of Colloidal Nanomaterials." *Met. Mater.-Int.* 8: 423.
- [20] Chang, J. F., Young, T. F., Yang, Y. L., Ueng, H. Y., and Chang, T. C. 2004. "Atomic Force Microscopy Study of the Kinetic Roughening in Nanostructured Gold Films on SiO₂." *Mater. Chem. Phys.* 83: 199.